SYNTHESIS, STRUCTURAL, MORPHOLOGICAL, OPTICAL AND ELECTRICAL STUDIES OF PANI / SnO_2 NANOCOMPOSITES

R. ANITHA[a], E. KUMAR[b,*], K. RATHNAKUMAR[c], S. C. VELLA DURAI[d]
[a]*Research scholar, Bharathiar University,Coimbatore, Tamilnadu, India; Sri S. Ramasamy Naidu Memorial College, Sattur, Virudhunagar, Tamilnadu, India*
[b]*Department of Physics, Tamil Nadu Open University, Chennai, Tamil Nadu, India*
[c]*Tamil Nadu Open University, Chennai, Tamil Nadu, India*
[d]*Department of Physics, JP College of Arts and science, Agarakattu, Tenkasi, Tirunelveli, Tamilnadu, India*

Tin Oxide (SnO_2) nanoparticles were prepared by the microwave-assisted solution method. Aniline monomers were prepared and polymerization in the suspension of SnO_2 to form nanocomposites material, in which SnO_2 nanoparticle was embedded within the polyaniline chain (PANI). Structural, Optical, Morphology and AC electrical conductivity studies of the sample were carried out using power X-ray diffraction, Fourier Transform Infrared Spectroscopy, UV-Vis Spectroscopy, Scanning Electron Microscope, High-Resolution Transmission Electron Microscope and AC Impedance Spectroscopy. Powder XRD helped to confirm the formation of PANI/SnO_2 composites and the crystallite size of the nanocomposite is found to be 16 nm. Structural changes of PANI due to the presence of SnO_2 in PANI/SnO_2 nanocomposites have been analyzed in FT-IR and UV-Vis spectrum. SEM images show the morphology of PANI/SnO_2 nanocomposites. HRTEM images were observed and showed that the SnO_2 was scattered and confirmed the PANI chain that formed a PANI/SnO_2 nanocomposites material. AC conductivity was studied in the frequency between 10 μHz - 8 MHz. At higher angular frequencies, the nanocomposites exhibit almost the maximum value of AC electrical conductivity (σ_{ac}) is found at 303K of SnO_2 in PANI.

(Received January 8, 2021; Accepted March 2, 2021)

Keywords: Conductivity, Frequency, PANI, Morphology, Nanocomposites

1. Introduction

In recent days, polyaniline has received more attention compared to other conducting polymers because of their very good potential applications like batteries, super capacitors, photovoltaic devices, and sensors, etc [1, 2]. Polyaniline (PANI) has attracted notable because of its high electrical conductivity, and very easy preparation methods [3]. PANI has some disadvantages like mechanical strength and low chemical stability that are unfortunate for related applications [4]. It has been published some articles that inorganic-organic hybrid material; it can complete the properties of pure inorganic or organic material. Therefore has been investigating to the PANI/Metal Oxide nanocomposites [5]. The combination of metal oxide with PANI to be a favorable try and at the same time improves the mechanical strength and stability of the PANI [6]. Some metal oxides like MnO_2, ZnO, RuO_2, TiO_2, and SnO_2 are used to forms composite with PANI [7]. Among those metal oxides, SnO_2 is an n-type semiconductor with broad the energy bandgap (Eg = 3.6 eV) at normal temperature and has much application like battery, solar cell, catalysis, and sensors [8]. So, PANI/SnO_2 nanocomposites have been analyzed by many research articles have prepared PANI/SnO_2 nanocomposites by in situ polymerization method [9]. These types of composite samples were found that the AC electrical conductivity showed a strong dependence on the wt% of metal oxide in PANI [10]. In this paper, we have discussed the synthesis of preparation of PANI / SnO_2 nanocomposites with five weight percentages (5wt%) and

* Corresponding author: kumarnano@gmail.com

various characterization techniques namely, X-Ray Diffraction (XRD), Fourier Transform Infrared Spectroscopy (FTIR), UltraViolet-Visible Spectroscopy (UV-Visible), High-Resolution Transmission Electron Microscopy (HRTEM), Scanning Electron Microscopy (SEM) and conductivity studies. The experimental data obtained from various characterization techniques are presented and discussed in detail.

2. Materials and Methods

2.1. Materials

All the chemicals were pursued from AR grade and are used without further purification. Ammonium persulfate (APS) [$(NH_4)_2S_2O_8$] (RANBAXY fine chemicals Limited, India), Aniline (AR grade MERCK), Hydrochloric acid (AR grade MERCK), Stannic chloride dihydrate ($SnCl_2.2H_2O$) (AR grade LOBA) and Ammonia (NH_3) (AR grade MERCK) were used to prepare the nanoparticles. De ionized water was used for the entire procedure.

2.2. Synthesis of Polyaniline (PANI)

Initially Aniline monomer was distilled using cubic condenser for purification. Aniline was added with 2M Hydrochloric acid, drop by drop and kept in a magnetic stirrer for continuous stirring for about 20 minutes. Ammonium persulfate was dissolved in deionized water and the solution was added drop wise with the above mixture and kept at room temperature for one day. Then the solution was filtered and dried at room temperature. Polyaniline powder was obtained with dark green colour. The structure of polyaniline is shown in Figure. 1.

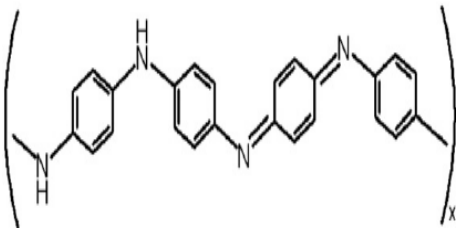

Fig. 1. Structure of Polyaniline.

2.3. Preparation of Tin Oxide Nanoparticles

The 3g of Stannous chloride dihydrate ($SnCl_2 \cdot 2H_2O$) were taken and then 5 ml ammonia were slowly mixed drop by drop, until its pH value raises upto 10. At that point the blend was kept in a stirrer for 0.5 hours, at 60^oC. This arrangement was kept in a microwave till the volume becomes one third of its initial volume. Soon after, it was cooled for three min and stirred continuously. So as to eliminate the polluting influences, the arrangement was washed 2 - 3 multiple times with deionized water. To eliminate the dampness content the wet nanoparticle was dried in air for three days. The dried nanoparticles were grounded utilizing mortar.

2.4. Synthesis of PANI / SnO_2 Nanocomposites

PANI / SnO_2 (5wt%) nanocomposite was prepared by in-situ polymerization method [1] of aniline in the presence of prepared SnO_2 using APS as an oxidant. 0.1M purified Aniline was added drop by drop with 2 M Hcl and the mixture were kept in a magnetic stirrer for 0.5 hours at 40^0C. Ammonium persulfate was dissolved in 2M Hcl solution and stirred for one hours. Then both the mixture was added with prepared SnO_2 nanoparticles with five weight percentage. The mixture solution was stirred continuously for 10 min. The colloidal solution obtained was cooled for one day. After cooling, it was filtered with whattsman filter paper and washed with deionized water for 2-3 times. In order to remove the moisture content, the wet nanocomposites were dried at room temperature for 3 days. The dried powder was grounded using pestle and mortar.

2.5. Characterization Techniques

The crystal structure of the PANI / SnO_2 nanocomposites were investigated by X-Ray Diffraction (XRD) technique and the data were recorded using an X-ray diffractometer (Model Bruker D8) with Nickel filtered Cu - Kα radiation. Data were collected in the range of 2θ from 10^o to 80^o using step scan mode with step size of 0.0170° and step time of 1.0000s. FT-IR spectra of the sample were recorded in the range of 400 – 4000cm^{-1}, using a Shimadzu 8400S FT-IR Spectrometer. Ultraviolet-Visible spectra of PANI / SnO_2 nanocomposites were recorded using UV – 1800 series spectrophotometer in the absorption mode. The ultraviolet (UV) region scanned is normally from 200 to 400nm and the visible portion is from 400 to 800 nm. SEM images of PANI / SnO_2 nanocomposites were recorded using the Model Hitachi SEM S 2400 device at SAIF-STIC, CUSAT, Cochin. Microstructural analysis were made by HRTEM (MODEL - JOEL - J2000), operating at 200KV at SAIF-NEHU, Shillong. The samples were characterized using impedance spectroscopy. An impedance bridge (Zahner IM6) was used to measure the dielectric constants, impedance and ac conductivity at several frequencies in the range of 10μHz to 8MHz.

3. Results and Discussion

3.1. X-Ray Diffraction studies

The PANI / SnO_2 nanocomposites were characterized by X-Ray Diffraction technique (XRD) to find the structure and phase. The XRD image of PANI / SnO_2 (5wt%) nanocomposites are shown in Fig. 2. The XRD pattern of PANI / SnO_2 nanocomposites showed some peaks. From the peaks, crystallite size of nanocomposites was calculated using the FWHM(β) from the most intense XRD peak using scherrer formula [11]. The characteristic peaks of PANI / SnO_2(5wt%) nanocomposite were 26.6^0, 33.9^0, 51.8^0 which corresponds to the miller indices (1 1 0), (1 0 1) and (2 1 1) and it is similar to that of SnO_2, which matches well with JCPDS card No.41–1445 [12]. The XRD pattern of prepared nanocomposites showed that the sample was tetragonal rutile structure. The crystalline size for PANI / SnO_2 was found to be calculated as around 16 nm.

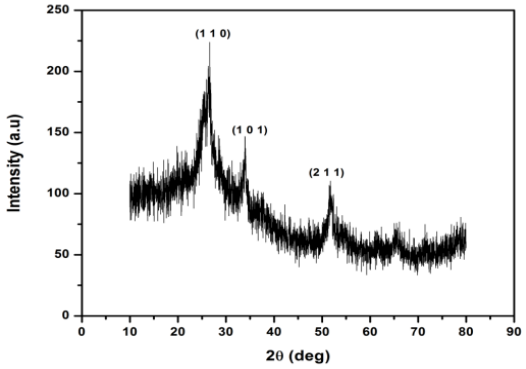

Fig. 2. XRD pattern of PANI / SnO_2 nanocomposite.

3.2. FT-IR Spectroscopic studies

The FT-IR spectra of PANI / SnO_2 nanocomposites shown by shown in Fig. 3. The peaks at 616.7 cm^{-1}corressponds [13] to the anti-symmetric Sn-O-Sn mode. Strong peaks at 613 cm^{-1} in both the samples are due to the anti-symmetric Sn-O-Sn mode in SnO_2, which confirms the presence of SnO_2 in the PANI matrix. Dutta et al [14] measured same result for PANI/SnO_2 nanocomposites [15]. The vibration band around 1550-1650cm^{-1} [13] is due to the C-N stretching vibration of quinoid rings whereas the vibration band around 1439-1498 cm^{-1} [13] arises due to the C-N stretching vibration associated with the benzenoid ring.

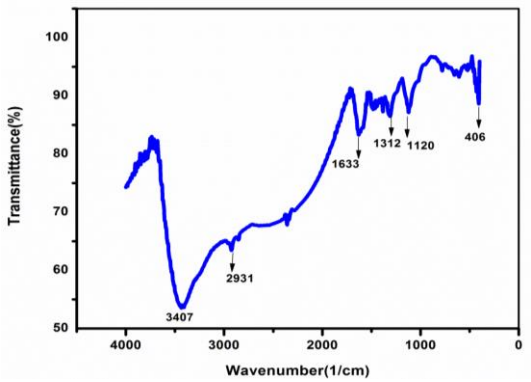

Fig. 3. FT-IR spectrum of PANI / SnO_2 nanocomposite.

3.3. UV – Visible Spectroscopic studies

The UV–Visible absorption spectrum and Tauc plot of the nanocomposites are shown in Fig. 4 & 5. From the Fig. 4, it was observed that there was an absorption band from 252nm to 349nm in the UV region, which was red shifted compared with the absorption peak of SnO_2 nanoparticles. The maximum absorption was found to be at 305nm for this nanocomposite. Another absorption band was also observed from 351nm to 490nm and the maximum absorption was found to be at 435nm. The band gap of PANI / SnO_2 nanocomposites were calculated from the Tauc plot and the calculated values of the band gap was 2.78eV for nanocomposites.

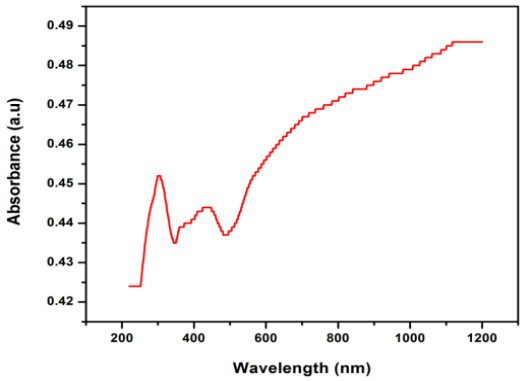

Fig. 4. UV–Visible absorption spectrum of PANI/SnO_2 (5wt%) nanocomposite.

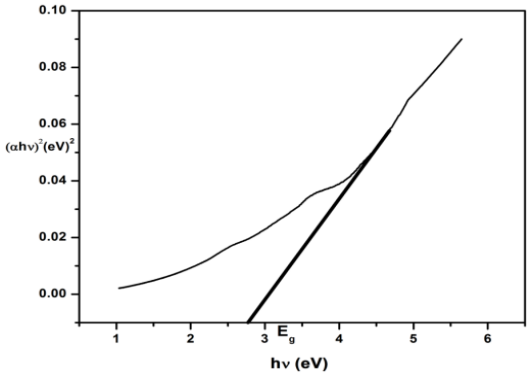

Fig. 5. Tauc plot of PANI / SnO_2 nanocomposite

Hence, as shown by UV–Visible Spectroscopy, during the maximum of weight % (5), the band gap value was low. Hence, the less band gap of the PANI / SnO_2 nanocomposites have been

attributed to the quantum confinement effect of the nanoparticles. The SnO_2 / PANI synthesized by Hemlata J. Sharma et al [16] shown in two characteristic peaks, one at 407 nm in visible region correspond to benzenoid to quinoid moieties showing polaron-π* transitions and other at 326 nm in UV corresponds to π-π* transitions of benzenoid ring and the insertion of SnO_2 in PANI. According to Manawwer Alam [17], the UV spectrum shows the absorption around 300 nm and the estimated energy bandgap was 4.1 eV. Three absorptions peak were measured in the spectra of PANI at 275, 371, 574 nm wavelength, which were attributed to p–p* conjugated ring systems, polaron-p* and p-polaron benzenoid to quinoid excitonic transition, respectively.

4.4. Morphological studies - Scanning Electron Microscope (SEM)

Fig. 6. Show the SEM images of PANI / SnO_2 at different magnification. The conducting polymers are highly sensitive towards temperature during the recording of SEM. When the sample interacts with electron it will generate certain amount of heat which may cause few cracks in the nanocomposite samples. It can be seen from the SEM images that the particles are well defined in the size ranging in nanometer level. It was also observed from the figures that the nanocomposites are highly dispersed with agglomeration. The aggregation of nanoparticles may be due to the effect of microwave heating because it forms the hot surface on primarily formed nanoparticles.

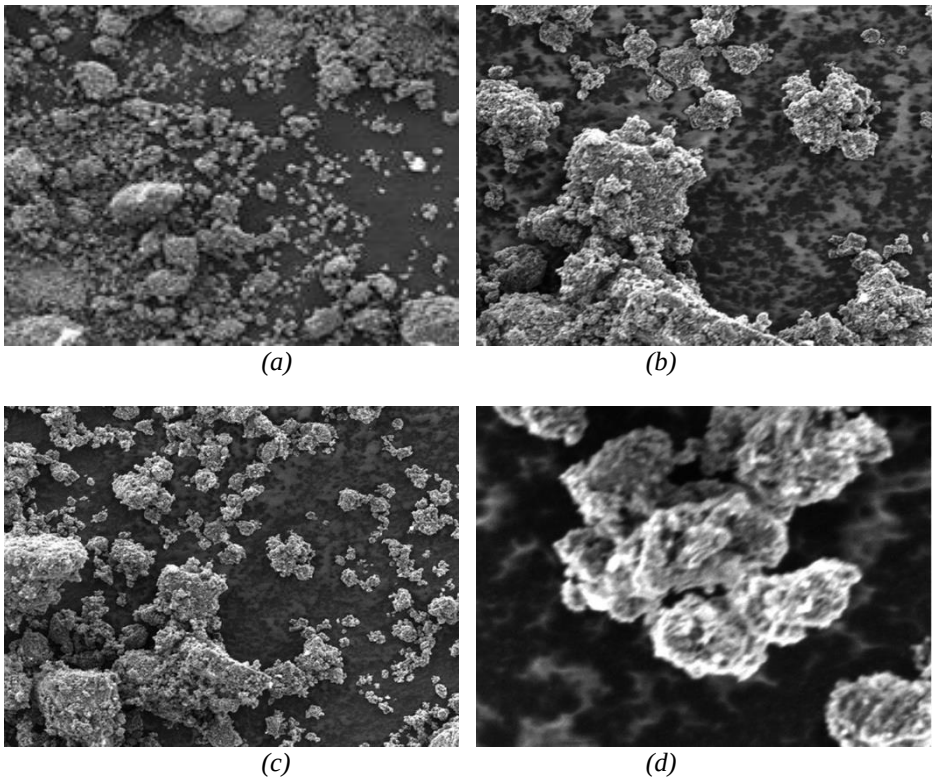

(a) *(b)*

(c) *(d)*

Fig. 6. (a), (b), (c) & (d) SEM image of PANI / SnO_2 nanocomposite.

The formation of polymer shell around the nanocrystalline particles can be seen in SEM images. Also, most of the particles of the samples are spherical in shape and slightly agglomerated. The SEM image of SnO_2 nanoparticles synthesized by L. I. Nadaf et al [18] shows that the homogeneous distribution of spherical particles. The SEM images of nanocomposite in which the grain is irregular in shape and the SnO_2 oxide partilcles are not well dispersed. According to A. A. Matnishyan et al [13], the SEM micrographs show high homogeneity of the nano material consisting of homogeneous nanocomposite and a globular particle is produced with inclusion of higher formation of PANI globules with sizes in the range of 30–50 nm.

3.5. Morphological studies - High Resolution Transmission Electron Microscope (HRTEM)

The morphology and particle size of PANI / SnO_2 nanocomposites were observed using HRTEM micrographs as shown in Fig. 7. The presence of irregular shaped nanocomposites as well as regular rod-like shaped and irregular rod-like shaped nanocomposites was observed in the HRTEM micrographs. The HRTEM micrographs confirmed the formation of PANI / SnO_2 nanocomposites. The SAED image of the PANI / SnO_2 nanocomposites are shown in Fig.7 and the bright spots in this image confirmed the crystallite nature of the nanocomposites. The calculated particle size from XRD investigation matches well with the particle size measured from HRTEM micrograph. Thus, it was clear from HRTEM analysis that the particle size increases with the increase in weight% which agrees well with the XRD results. The TEM micrographs of the nanocomposites synthesized by Danielle C. Schnitzler etal [19] observed the tubular morphology.

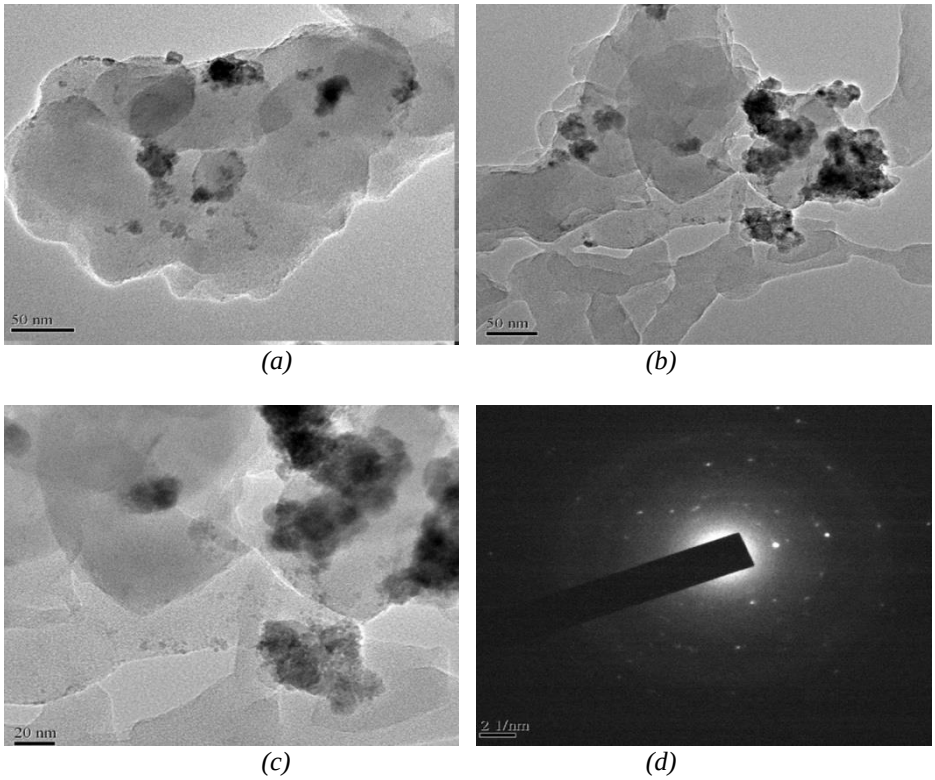

(a) *(b)*

(c) *(d)*

Fig. 7. (a), (b) & (c) HRTEM image of PANI/SnO_2 nanocomposite, (d) SAED pattern of PANI/SnO_2 nanocomposite.

3.6. Electrical studies - ac conductivity

The conductivity properties of PANI / SnO_2 nanocomposites can be explained as a function of frequency of the applied electric field. The ac conductivity measurements were made for PANI / SnO_2 nanocomposites at different temperatures for the frequency range between 10μHz and 8MHz. The ac conductivity (σ_{ac}) of the nanocomposites were calculated using the formula[20, 21],

$$\sigma_{ac} = \boldsymbol{\varepsilon_0}\ \boldsymbol{\varepsilon_r}\ \omega \tan\delta$$

where ε_0 is the permittivity of free space (8.85×10^{-12} Farad/metre), $\boldsymbol{\varepsilon_r}$ is the dielectric constant, $\omega(2\pi f)$ is the angular frequency and $\tan\delta$ is the loss factor.

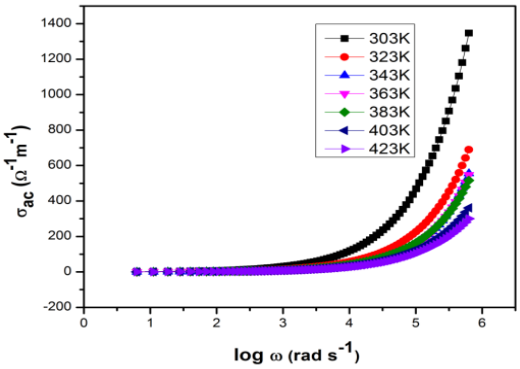

Fig. 8. Variation of ac conductivity with frequency of PANI / SnO_2 nanocomposite.

Fig. 8. shows the variation of ac conductivity with varying frequency for PANI / SnO_2 nanocomposites at different temperatures. The ac conductivity strongly depends on frequency and the conductivity was found to increase at higher frequency region. It was observed that the ac conductivity remains almost constant upto 1 KHz. Above 1KHz, it increases gradually upto 40 KHz and then increases rapidly from 40KHz – 620KHz. i.e., at low frequency region, there was a smaller increase in the electrical conductivity of the nanocomposite, whereas at high frequency region, there was a rapid increase in the conductivity. Hence, it was observed the ac conductivity strongly depends on frequency and the conductivity was found to be high at higher frequencies.

4. Conclusion

The structural parameters of the PANI / SnO_2 nanocomposites namely, crystallite size was calculated using XRD technique. The XRD pattern of PANI / SnO_2 nanocomposites showed that the prepared samples were tetragonal rutile structure. The functional groups of PANI / SnO_2 nanocomposites were identified from FT-IR spectra. The UV-Visible absorption spectrum of PANI / SnO_2 nanocomposites was recorded. The band gap energy of all the samples was calculated from Tauc plots. The high resolution transmission electron micrographs indicate that the PANI / SnO_2 nanocomposites were formed with particle size which matches with that of XRD results.

From the HRTEM micrographs, it was observed that particles were formed with particle size of around 16nm. The presence of regular and irregular rod-like shaped PANI / SnO_2 nanocomposites was also observed. The SEM images of the powdered samples revealed that the PANI / SnO_2 nanocomposites formed are highly dispersed with agglomeration. In PANI / SnO_2 nanocomposite, SnO_2 nanoparticles are surrounded by polyaniline matrix. AC electrical conductivities studies of all the samples showed the frequency dependence conductivity behavior of PANI / SnO_2 nanocomposites.

References

[1] Z. Li, L. Gong, Materials **13**(3), 548 (2020).
[2] S. C. Vella Duraia, E. Kumar, Journal of Ovonic Research **16**(3), 173(2020).
[3] H. Wang, J. Lin Z. X. Shen, Journal of Science: Advanced Materials and Devices **1**(3), 225(2016).
[4] P. Marcasuzaa, S. Reynaud, F. Ehrenfeld, A. Khoukh, J. Desbrieres, Biomacromolecules **11**(6), 1684(2010).
[5] L. Geng, S. Wu, Materials Research Bulletin **48**(10), 4339 (2013).
[6] S. Vyas, S. Shivhare, A. Shivhare, International Journal of Research and Scientific Innovation **4**(7), 86 (2017).

[7] S. C. Vella Durai, E. Kumar, D. Muthuraj, V. Bena Jothy, International Journal of Nano Dimension **10**(4), 410 (2019).
[8] M. Periyasamy, A. Kar, Journal of Materials Chemistry C **8**(14), 4604 (2020).
[9] L. Sun, Y. Shi, Z. He, B. Li, J. Liu, Synthetic Metals **162**(24), 2183 (2012).
[10] S. Kalyane, U. V. Khadke, International Journal of Pure and Applied Physics **13**(2), 201 017).
[11] J. E. Ghoula, G. A. Khouqeer, Journal of Ovonic Research **16**(5), 273 (2020).
[12] N. G. Deshpande, Y. G. Gudage, R. Sharma, J. C. Vyas, J. B. Kim, Y. P. Lee, Sensors and Actuators B **138**, 76 (2009).
[13] A. A. Matnishyan, T. L. Akhnazaryan, G. V. Abaghyan, S. I. Petrosyan, G. R. Badalyan, M. G. Eghikyan, Journal of Contemporary Physics **45**, 246 (2010).
[14] K. S. K. Dutta, S. K. De, Material Letters **61**, 4967 (2007).
[15] S. B. Kondawar, S. P. Agrawal, S. H. Nimkar, H. J. Sharma, P. T. Patil, Advanced Material Letters **3**(5), 393 (2012).
[16] H. J. Sharma, D. V. Jamkar, S. B. Kondawar, International Journal of Science and Research, International Symposium on Ultrasonics **2015**, 22(2015).
[17] M. Alam, A. A. Ansari, M. R. Shaik, N. M. Alandis, Arabian Journal of Chemistry **6**, 341 013).
[18] L. I. Nadaf, K. S. Venkatesh, M. A. Gadyal, M. Afzal, IOSR Journal of Applied Chemistry **9**, 55 2016).
[19] D. C. Schnitzler, M. S. Meruvia, I. A. Hummelgen, A. J. G. Zarbin, Chemistry of Materials **15**, 4658 (2003).
[20] S. C. Vella Durai , E. Kumar , R. Indira , D. Muthuraj, Journal of Ovonic Research **16**(6), 345 (2020).
[21] S. A. Gad, A. M. Moustafa, A. A. Azab, A. F. Hega, Journal of Ovonic Research **16**(5), 293 (2020).